PERGAMON

International Journal of Solids and Structures 39 (2002) 159–174

INTERNATIONAL JOURNAL OF SOLIDS and STRUCTURES

www.elsevier.com/locate/ijsolstr

A variational method for unidirectional fiber-reinforced composites with matrix creep

N. Ohno [a,*], T. Ando [a], T. Miyake [b], S. Biwa [a]

[a] *Department of Mechanical Engineering, School of Engineering, Nagoya University, Furo-cho, Chikusa-ku, Nagoya 464-8603, Japan*
[b] *Nagoya Municipal Industrial Research Institute, Rokuban, Atsuta-ku, Nagoya 456-0058, Japan*

Received 10 October 2000; in revised form 31 May 2001

Abstract

A variational method is developed for analyzing the matrix creep induced time-dependent change in fiber stress profiles in unidirectional composites. A functional of admissible profiles of fiber stress rate is presented by supposing a fiber broken in matrix as well as a fiber pulled out from matrix. The functional is shown to have the stationary function satisfying an incremental differential equation based on the shear lag assumption. Then, the stationary function is approximately determined by assuming bilinear profiles of fiber stress and a power law of matrix creep, leading to analytical solutions for the time-dependent change in fiber stress profiles. The solutions are verified on the basis of an energy balance equation and a finite difference computation. Moreover, it is shown that the solution for the fiber pull-out model agrees well with an experiment on a single carbon fiber/acrylic model composite if the initial slip at fiber/matrix interface is taken into account. In addition, the solution for the fiber breakage model is used for evaluating the characteristic time in long-term creep rupture of unidirectional composite.

Keywords: Variational method; Fiber-reinforced composite; Matrix creep; Time-dependent change; Shear lag theory

1. Introduction

Unidirectional composites reinforced with long brittle fibers may suffer from fiber breaks. In the broken fibers, fiber stress is zero at the breaks but recovers the stress in intact fibers as axial distance increases from each break. The distance for such a transient change in fiber stress is called the stress recovery, or transfer, length and is important for evaluating the longitudinal tensile strength of composites.

Matrix creep may occur in metal matrix and polymer matrix composites. Then, the profiles of fiber stress in broken fibers change with time, even if stress applied to composites is constant. This time-dependent change causes the stress transfer length to increase with time, so that the carrying load of broken fibers reduces; then, since the carrying load of intact fibers increases, further fiber breaks may occur to induce

* Corresponding author. Tel.: +81-52-789-4475; fax: +81-52-789-5131.
E-mail address: ohno@mech.nagoya-u.ac.jp (N. Ohno).

0020-7683/01/$ - see front matter
PII: S0020-7683(01)00147-0

eventually the creep rupture of composites (Lifshitz and Rotem, 1970; Phoenix et al., 1988; Otani et al., 1991; Ohno et al., 1994a,b).

Hence, the effect of matrix creep on the stress profiles in broken fibers is a fundamental subject, but analytical solutions have been obtained only in a few cases: Lifshitz and Rotem (1970) derived approximately a linear viscoelastic solution for an axisymmetric cell containing a broken fiber by utilizing the Laplace transformation. Mason et al. (1992) succeeded in obtaining an exact solution for a 2D plate model by assuming the power-law creep of matrix, although they ignored the elastic strain of matrix. For an axisymmetric model with nonlinear matrix creep, Iyengar and Curtin (1997) evaluated approximately but analytically the time-dependent extension of the stress transfer length on the basis of the numerical study of Du and McMeeking (1995). However, their analytical evaluation was restricted to only three integers of the stress exponent of matrix creep, as they did not ignore the elastic strain of matrix. Thus it is worthwhile to attain more generally applicable, analytical solutions, in which both the elastic and nonlinear creep strains of matrix are taken into account.

The solutions mentioned above were obtained by solving differential equations based on the shear lag assumption. It is, however, possible to utilize a variational method if a functional is known for the problem considered. Variational methods are effective especially if the forms of solutions can be assumed appropriately. The methods enable us to obtain approximate solutions most accurately within the assumed forms of solutions, since the unknown coefficients in assumed solutions are determined rationally by getting the functionals stationary. For the elastic-creep problems of unidirectional fiber composites, however, variational methods have not been utilized yet.

The time-dependent change in fiber stress profiles can occur in a fiber pulled out from matrix as almost equally as in a fiber broken in matrix, because these two problems are governed by essentially the same equations (see Mason et al., 1992). It is, however, much easier to perform constant-load pull-out tests on single-fiber model composites for the purpose of utilizing laser Raman spectroscopy for observing the effect of matrix creep on fiber stress profiles (Miyake et al., 2001). It is, therefore, worthy developing a variational method and deriving analytical solutions of both the fiber breakage and fiber pull-out problems. For such problems, it is in general necessary to take into account the radial variation of matrix shear stress (Clyne and Withers, 1993); the radial variation is essential for analyzing single-fiber model composites (Li and Grubb, 1994).

Ohno and Miyake (1999) considered an energy approach to discuss analytically the time-dependent change in fiber stress profiles in broken fibers. This approach is based on the energy balance that the elastic energy released from a broken fiber is dissipated due to matrix creep around the fiber break. Thus, they obtained an approximate solution for the time-dependent extension of the stress transfer length, though the elastic strain of matrix and the radial variation of matrix shear stress were ignored. Then, using the resulting solution as well as Curtin's (1991) model, they estimated analytically the long-term creep rupture time and strain of unidirectional composites. Useful findings were thus attained such as the dependence of rupture time on applied stress. Nevertheless, it is open to obtain analytical solutions of the fiber pull-out problem with the effect of matrix creep. Moreover, it is of significance to discuss whether the energy-balance based solution mentioned above is derivable from a variational method, the principle of which has been well established.

In this work, the time-dependent increase of the stress transfer length will be analyzed analytically by developing a variational method for fiber breakage and fiber pull-out axisymmetric models, in which both the elastic and creep strains of matrix as well as the radial variation of matrix shear stress will be taken into account. First, a functional based on incremental complementary energy will be demonstrated for the axisymmetric models, and it will be shown that the functional has a stationary function, which satisfies a shear lag differential equation. Second, by supposing bilinear profiles of fiber stress and the power-law creep of matrix, approximate solutions will be derived for the time-dependent increase of the stress transfer length, and it will be discussed whether the resulting solutions satisfy the energy balance considered by

Ohno and Miyake (1999). Third, the solution for the fiber pull-out model will be compared with a finite-difference computation of the shear lag equation and with one of the laser Raman spectroscopic experiments done by Miyake et al. (1998, 2001). Finally, the solution for the fiber breakage model will be employed for evaluating the characteristic time in the long-term creep rupture of unidirectional composites analyzed by Ohno and Miyake (1999).

2. Axisymmetric shear lag models

In the present work, we consider two kinds of axisymmetric models based on the shear lag assumption, i.e., a fiber breakage model and a fiber pull-out model. To begin with, we describe the models briefly.

In the fiber breakage model, a broken fiber of a radius r_f is embedded in matrix in a cell, which has an outer radius R and an axial length 2ℓ (Fig. 1). Let us denote radial and axial coordinates by r and z, respectively. We suppose that the lateral surface of the cell contacts with intact fibers, and so that the cell is subjected to uniform, axial strain $\varepsilon(t)$ at the outer peripheral and at the axial ends (Lifshitz and Rotem, 1970; Du and McMeeking, 1995; Iyenger and Curtin, 1997; Ohno and Miyake, 1999):

$$\frac{\partial u}{\partial z} = \varepsilon(t) \quad \text{at } r = R, \tag{1}$$

$$\frac{\partial u}{\partial z} = \varepsilon(t) \quad \text{at } z = \pm\ell, \tag{2}$$

where t indicates time, and u denotes axial displacement.

Employing the shear lag assumption (Cox, 1952), we regard the fiber as a 1D bar and consider only the shear deformation in matrix to be responsible for the distribution of fiber stress. Then, if Hooke's law is assumed for the broken fiber, we have

$$\frac{\partial u_f}{\partial z} = \frac{\sigma_f}{E_f}, \tag{3}$$

where u_f and σ_f signify the axial displacement and axial stress in fibers, respectively, and E_f indicates Young's modulus of fibers. The fiber stress σ_f is related with the shear stress acting on the fiber/matrix interface, τ_i, as

$$\tau_i = -\frac{r_f}{2}\frac{\partial \sigma_f}{\partial z}. \tag{4}$$

If the matrix exhibits creep in addition to elastic deformation, the shear strain rate in matrix, $\dot{\gamma}_m$, has an expression

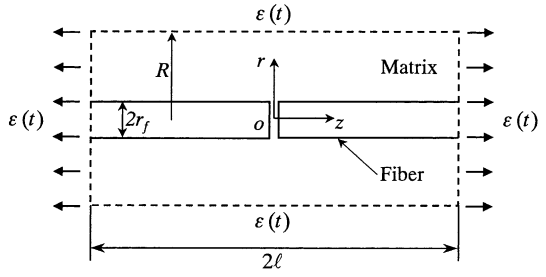

Fig. 1. Axisymmetric cell consisting of broken fiber and elastic-creeping matrix subjected to overall strain $\varepsilon(t)$.

$$\dot{\gamma}_m = \frac{\dot{\tau}_m}{G_m} + \dot{\gamma}_m^{\mathrm{c}}, \tag{5}$$

where τ_m and $\dot{\gamma}_m^{\mathrm{c}}$ represent the shear stress and shear creep rate in matrix, respectively, and G_m denotes the elastic shear rigidity of matrix. The superposed dot stands for the differentiation with respect to time t. In the model, $\dot{\gamma}_m$ may satisfy accurately $\dot{\gamma}_m = \partial\dot{u}/\partial r$, so that using the above equation we can have

$$\dot{u}_R - \dot{u}_{\mathrm{f}} = \int_{r_{\mathrm{f}}}^{R} \left(\frac{\dot{\tau}_m}{G_m} + \dot{\gamma}_m^{\mathrm{c}} \right) \mathrm{d}r, \tag{6}$$

where u_R denotes u at $r = R$.

In the present work, since the difference between R and r_{f} cannot be small, we take into account the radial variation of τ_m in matrix by assuming the following self-equilibrium equation of τ_m in matrix (Clyne and Withers, 1993; Li and Grubb, 1994):

$$r\tau_m = r_{\mathrm{f}}\tau_{\mathrm{i}}. \tag{7}$$

Then, Eq. (6) becomes

$$\dot{u}_R - \dot{u}_{\mathrm{f}} = \ln\frac{R}{r_{\mathrm{f}}}\,\frac{r_{\mathrm{f}}\dot{\tau}_{\mathrm{i}}}{G_m} + \int_{r_{\mathrm{f}}}^{R} \dot{\gamma}_m^{\mathrm{c}}\,\mathrm{d}r. \tag{8}$$

Differentiating the above equation with respect to z, and using Eqs. (1), (3) and (4), we obtain

$$\frac{r_{\mathrm{f}}^2}{2G_m}\ln\frac{R}{r_{\mathrm{f}}}\,\frac{\partial^2\dot{\sigma}_{\mathrm{f}}}{\partial z^2} - \frac{\dot{\sigma}_{\mathrm{f}}}{E_{\mathrm{f}}} - \int_{r_{\mathrm{f}}}^{R} \frac{\partial\dot{\gamma}_m^{\mathrm{c}}}{\partial z}\,\mathrm{d}r + \dot{\varepsilon}(t) = 0, \tag{9}$$

which is a differential equation for $\dot{\sigma}_{\mathrm{f}}(z,t)$ subjected to boundary conditions

$$\sigma_{\mathrm{f}}(0,t) = 0, \tag{10}$$

$$\sigma_{\mathrm{f}}(\pm\ell,t) = E_{\mathrm{f}}\varepsilon(t). \tag{11}$$

It is obvious that Eq. (9) is applicable to the fiber pull-out model shown in Fig. 2. For this model, we assume that the hatched part in the figure has no strain, so that in Eq. (9)

$$\varepsilon(t) = 0. \tag{12}$$

Moreover, the boundary conditions are

$$\sigma_{\mathrm{f}}(0,t) = p(t), \tag{13}$$

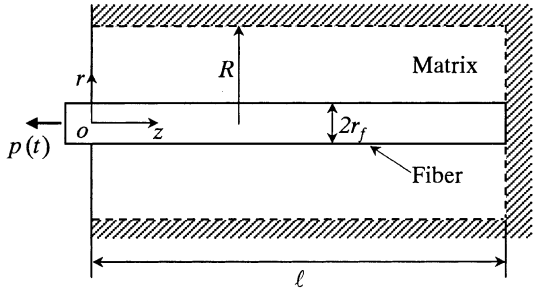

Fig. 2. Axisymmetric model for pull-out of fiber embedded in elastic-creeping matrix.

$$\sigma_{\mathrm{f}}(\ell, t) = 0, \tag{14}$$

where $p(t)$ indicates the pull-out force per unit area of the fiber.

If only elastic deformation takes place in the matrix at $t = 0$, the following shear lag equation is applicable to the initial states in the two models mentioned above:

$$\frac{r_{\mathrm{f}}^2}{2G_m} \ln\frac{R}{r_{\mathrm{f}}} \frac{\mathrm{d}^2\sigma_{\mathrm{f}}}{\mathrm{d}z^2} - \frac{\sigma_{\mathrm{f}}}{E_{\mathrm{f}}} + \varepsilon_0 = 0, \tag{15}$$

where $\varepsilon_0 = \varepsilon(0)$, and $\varepsilon_0 = 0$ for the fiber pull-out model.

3. Functional and stationary function

For the two kinds of axisymmetric models described in the preceding section, it has been assumed that fibers are regarded as 1D bars deforming uniaxially, and that only the shear deformation in matrix has influence on the axial distribution of fiber stress. In accordance with this shear lag assumption, now let us consider an incremental complementary energy function

$$U = \pi r_{\mathrm{f}}^2 \int_0^{\ell} \frac{\dot{\sigma}_{\mathrm{f}}^2}{2E_{\mathrm{f}}}\,\mathrm{d}z + 2\pi \int_0^{\ell}\int_{r_{\mathrm{f}}}^{R} \left(\frac{\dot{\tau}_m^2}{2G_m} + \dot{\tau}_m \dot{\gamma}_m^{\mathrm{c}}\right) r\,\mathrm{d}r\,\mathrm{d}z - 2\pi R \int_0^{\ell} \dot{\tau}_R \dot{\varepsilon} z\,\mathrm{d}z, \tag{16}$$

where τ_R stands for τ_m at $r = R$. In the right-hand side of the above equation, the first term represents the incremental elastic energy in the fiber embedded in matrix, the second term the incremental elastic energy and energy dissipation induced by the shear stress in matrix, and the third term the variation in incremental complementary energy due to the uniform, axial strain rate $\dot{\varepsilon}(t)$ at $r = R$. It is emphasized that the second term deals with only the shear in matrix in conformity with the shear lag assumption.

Using Eqs. (4) and (7), we obtain

$$\tau_m(r, z, t) = -\frac{r_{\mathrm{f}}^2}{2r} \frac{\partial\sigma_{\mathrm{f}}(z, t)}{\partial z}. \tag{17}$$

Substitution of the above equation into Eq. (16) allows the incremental complementary energy U to become a functional of $\dot{\sigma}_{\mathrm{f}}(z, t)$:

$$U[\dot{\sigma}_{\mathrm{f}}(z, t)] = \pi r_{\mathrm{f}}^2 \int_0^{\ell} F(z, \dot{\sigma}_{\mathrm{f}}, \dot{\sigma}'_{\mathrm{f}})\mathrm{d}z, \tag{18}$$

where $\sigma'_{\mathrm{f}} = \partial\sigma_{\mathrm{f}}/\partial z$, and

$$F = \frac{\dot{\sigma}_{\mathrm{f}}^2}{2E_{\mathrm{f}}} + \frac{r_{\mathrm{f}}^2}{4G_m} \ln\frac{R}{r_{\mathrm{f}}} \dot{\sigma}_{\mathrm{f}}'^2 - \dot{\sigma}'_{\mathrm{f}} \int_{r_{\mathrm{f}}}^{R} \dot{\gamma}_m^{\mathrm{c}}\,\mathrm{d}r + \dot{\sigma}'_{\mathrm{f}} \dot{\varepsilon} z. \tag{19}$$

The boundary conditions for $\dot{\sigma}_{\mathrm{f}}(z, t)$ in Eq. (18) are

$$\dot{\sigma}_{\mathrm{f}}(0, t) = \dot{p}(t), \tag{20}$$

$$\dot{\sigma}_{\mathrm{f}}(\ell, t) = E_{\mathrm{f}} \dot{\varepsilon}(t). \tag{21}$$

Here it is noted that $p(t) = 0$ in the fiber breakage model, and that $\varepsilon(t) = 0$ in the fiber pull-out model.

The stationary function of the above functional U satisfies Euler's equation

$$\frac{\partial F}{\partial \dot{\sigma}_{\mathrm{f}}} - \frac{\mathrm{d}}{\mathrm{d}z}\left(\frac{\partial F}{\partial \dot{\sigma}'_{\mathrm{f}}}\right) = 0. \tag{22}$$

Substitution of Eq. (19) into Eq. (22) yields

$$\frac{r_f^2}{2G_m}\ln\frac{R}{r_f}\frac{\partial^2\dot{\sigma}_f}{\partial z^2}-\frac{\dot{\sigma}_f}{E_f}-\int_{r_f}^{R}\frac{\partial\dot{\gamma}_m^c}{\partial z}\,dr+\dot{\varepsilon}(t)=0. \tag{23}$$

This is just Eq. (9), i.e., the shear lag differential equation given in the preceding section. Therefore, Eq. (9) can be solved equivalently by finding the stationary function of the functional U given by Eqs. (18) and (19).

If only elastic deformation takes place in the matrix at $t=0$, we can consider a complementary energy function

$$U=\pi r_f^2\int_0^{\ell}\frac{\sigma_f^2}{2E_f}dz+2\pi\int_0^{\ell}\int_{r_f}^{R}\frac{\tau_m^2}{2G_m}r\,dr\,dz-2\pi R\int_0^{\ell}\tau_R\varepsilon_0 z\,dz. \tag{24}$$

Substitution of Eq. (17) into the above equation gives a functional

$$U[\sigma_f(z,t)]=\pi r_f^2\int_0^{\ell}F(z,\sigma_f,\sigma_f')\,dz, \tag{25}$$

where

$$F=\frac{\sigma_f^2}{2E_f}+\frac{r_f^2}{4G_m}\ln\frac{R}{r_f}\sigma_f'^2+\sigma_f'\varepsilon_0 z. \tag{26}$$

Then, we can derive Eq. (15) by substituting Eq. (26) into the following Euler's equation relevant to Eq. (25):

$$\frac{\partial F}{\partial\sigma_f}-\frac{d}{dz}\left(\frac{\partial F}{\partial\sigma_f'}\right)=0. \tag{27}$$

4. Analytical solutions based on bilinear profiles of fiber stress

Fig. 3(a) and (b) schematically illustrate the profiles of fiber stress in the fiber breakage and fiber pull-out models, respectively. It may be simplest to approximate bilinearly the profiles, as indicated by the dashed lines in the figures. In the present section, adopting such a bilinear approximation, we will derive analytical solutions on the basis of the functional U demonstrated in the preceding section. Then, it will be examined whether the resulting solutions satisfy energy balance within the shear lag assumption.

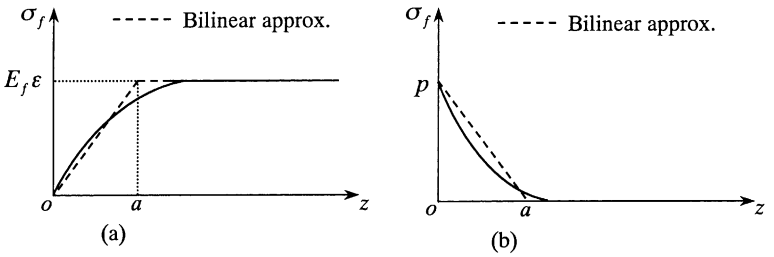

Fig. 3. Schematic illustration of fiber stress profile; (a) fiber breakage model and (b) fiber pull-out model.

4.1. Fiber pull-out model

Here we consider the fiber pull-out model first, since it is simpler. Let us suppose that the force applied to the fiber is constant (i.e., $p(t) = p_0$), and let us approximate bilinearly $\sigma_f(z,t)$ in the fiber pull-out model as

$$\sigma_f(z,t) = \begin{cases} p_0[1 - z/a(t)], & 0 \leqslant z \leqslant a, \\ 0, & a \leqslant z \leqslant \ell, \end{cases} \tag{28}$$

where $a(t)$ denotes a stress transfer length (Fig. 3(b)). Then, $\dot{\sigma}_f(z,t)$ has an expression

$$\dot{\sigma}_f(z,t) = \begin{cases} p_0 z\dot{a}(t)/a^2, & 0 \leqslant z \leqslant a, \\ 0, & a \leqslant z \leqslant \ell. \end{cases} \tag{29}$$

Substituting Eq. (29) into the functional U given by Eqs. (18) and (19), we obtain

$$U = \frac{\pi r_f^2 p_0}{a}\left[p_0\dot{a}^2\left(\frac{1}{6E_f} + \frac{r_f^2}{4G_m a^2}\ln\frac{R}{r_f}\right) - \frac{\dot{a}}{a}\int_0^a\int_{r_f}^R \dot{\gamma}_m^c \,\mathrm{d}r\,\mathrm{d}z\right]. \tag{30}$$

As was represented in Eq. (18), formulation of the present variational method is incremental. Accordingly, the above functional U should be taken to be stationary with respect to $\dot{a}$ by supposing that the current value of a is known. Thus, using

$$\frac{\partial U}{\partial \dot{a}} = 0, \tag{31}$$

we obtain

$$p_0\left(\frac{1}{3E_f} + \frac{r_f^2}{2G_m a^2}\ln\frac{R}{r_f}\right)\dot{a} - \frac{1}{a}\int_0^a\int_{r_f}^R \dot{\gamma}_m^c \,\mathrm{d}r\,\mathrm{d}z = 0. \tag{32}$$

In the fiber pull-out model, τ_m is the dominant stress in matrix. Thus, if we assume for simplicity Norton's law for $\dot{\gamma}_m^c$, we can have

$$\dot{\gamma}_m^c = B_\tau|\tau_m|^{n-1}\tau_m, \tag{33}$$

where B_τ and n are material constants. Substitution of Eqs. (17) and (28) into Eq. (33) gives

$$\dot{\gamma}_m^c = B_\tau\left(\frac{r_f^2 p_0}{2ar}\right)^n. \tag{34}$$

Then, since Eq. (32) results in

$$\left(\frac{a^n}{3E_f} + \frac{r_f^2 a^{n-2}}{2G_m}\ln\frac{R}{r_f}\right)\dot{a} = \frac{B_\tau r_f^{2n} p_0^{n-1}}{2^n}\int_{r_f}^R \frac{\mathrm{d}r}{r^n}, \tag{35}$$

we obtain an analytical solution

$$\frac{a(t)^2 - a(0)^2}{3E_f} + \frac{r_f^2}{G_m}\ln\frac{R}{r_f}\ln\frac{a(t)}{a(0)} = B_\tau r_f^2\ln\frac{R}{r_f}t, \quad n = 1, \tag{36a}$$

$$\frac{a(t)^{n+1} - a(0)^{n+1}}{3(n+1)E_f} + \frac{r_f^2\ln(R/r_f)[a(t)^{n-1} - a(0)^{n-1}]}{2(n-1)G_m} = \frac{B_\tau r_f^{n+1} p_0^{n-1}}{2^n(n-1)}\left[1 - \left(\frac{r_f}{R}\right)^{n-1}\right]t, \quad n \neq 1. \tag{36b}$$

The initial value $a(0)$ in the above solution can be evaluated using the elastic functional (25) as follows: Substitution of Eq. (28) and $\varepsilon_0 = 0$ into Eq. (25) with Eq. (26) provides

$$U = \pi r_{\mathrm{f}}^2 p_0^2 \left(\frac{a}{6E_{\mathrm{f}}} + \frac{r_{\mathrm{f}}^2}{4G_m a} \ln \frac{R}{r_{\mathrm{f}}} \right). \tag{37}$$

Then, using

$$\frac{\mathrm{d}U}{\mathrm{d}a} = 0, \tag{38}$$

we obtain

$$a(0) = r_{\mathrm{f}} \left(\frac{3E_{\mathrm{f}}}{2G_m} \ln \frac{R}{r_{\mathrm{f}}} \right)^{1/2}. \tag{39}$$

4.2. Fiber breakage model

An analytical solution for the fiber breakage model can be derived in almost the same way, if overall strain $\varepsilon(t)$ is constant (i.e., $\varepsilon(t) = \varepsilon_0$). For this model, $\sigma_{\mathrm{f}}(z,t)$ can be approximated bilinearly as

$$\sigma_{\mathrm{f}}(z,t) = \begin{cases} E_{\mathrm{f}}\varepsilon_0 z/a(t), & 0 \leqslant z \leqslant a, \\ E_{\mathrm{f}}\varepsilon_0, & a \leqslant z \leqslant \ell. \end{cases} \tag{40}$$

Then, Eqs. (18) and (19) give

$$U = \frac{\pi r_{\mathrm{f}}^2 E_{\mathrm{f}}\varepsilon_0}{a} \left[E_{\mathrm{f}}\varepsilon_0 \dot{a}^2 \left(\frac{1}{6E_{\mathrm{f}}} + \frac{r_{\mathrm{f}}^2}{4G_m a^2} \ln \frac{R}{r_{\mathrm{f}}} \right) + \frac{\dot{a}}{a} \int_0^a \int_{r_{\mathrm{f}}}^R \dot{\gamma}_m^{\mathrm{c}} \, \mathrm{d}r \, \mathrm{d}z \right]. \tag{41}$$

Hence, using Eq. (31), we obtain

$$E_{\mathrm{f}}\varepsilon_0 \left(\frac{1}{3E_{\mathrm{f}}} + \frac{r_{\mathrm{f}}^2}{2G_m a^2} \ln \frac{R}{r_{\mathrm{f}}} \right) \dot{a} + \frac{1}{a} \int_0^a \int_{r_{\mathrm{f}}}^R \dot{\gamma}_m^{\mathrm{c}} \, \mathrm{d}r \, \mathrm{d}z = 0. \tag{42}$$

In the fiber breakage model, the axial normal stress in matrix is as dominant as matrix shear stress τ_m in the initial state, in contrast to the fiber pull-out model. The axial normal stress in matrix, however, tends to relax much more quickly than τ_m as matrix creep proceeds (Du and McMeeking, 1995; Ohno and Miyake, 1999). Thus, we may assume Eq. (33) to express $\dot{\gamma}_m^{\mathrm{c}}$. Eq. (42) then can be integrated analytically as

$$\frac{a(t)^2 - a(0)^2}{3E_{\mathrm{f}}} + \frac{r_{\mathrm{f}}^2}{G_m} \ln \frac{R}{r_{\mathrm{f}}} \ln \frac{a(t)}{a(0)} = B_\tau r_{\mathrm{f}}^2 \ln \frac{R}{r_{\mathrm{f}}} t, \quad n = 1, \tag{43a}$$

$$\frac{a(t)^{n+1} - a(0)^{n+1}}{3(n+1)E_{\mathrm{f}}} + \frac{r_{\mathrm{f}}^2 \ln(R/r_{\mathrm{f}})[a(t)^{n-1} - a(0)^{n-1}]}{2(n-1)G_m} = \frac{B_\tau r_{\mathrm{f}}^{n+1} (E_{\mathrm{f}}\varepsilon_0)^{n-1}}{2^n (n-1)} \left[1 - \left(\frac{r_{\mathrm{f}}}{R} \right)^{n-1} \right] t, \quad n \neq 1. \tag{43b}$$

For the fiber breakage model, Eq. (25) with Eq. (26) is reduced to

$$U = \pi r_{\mathrm{f}}^2 (E_{\mathrm{f}}\varepsilon_0)^2 \left(\frac{a}{6E_{\mathrm{f}}} + \frac{r_{\mathrm{f}}^2}{4G_m a} \ln \frac{R}{r_{\mathrm{f}}} + \frac{\ell}{2E_{\mathrm{f}}} \right). \tag{44}$$

Hence, applying Eq. (38) to the above equation, we obtain again Eq. (39), which gives the initial value $a(0)$ in the solutions (43a) and (43b).

4.3. Energy balance

For the fiber pull-out model dealt with in Section 4.1, the external work done by pull-out force p_0 should be equal to the change rate of internal energy with respect to time:

$$\pi r_{\mathrm{f}}^2 p_0 \dot{\lambda} = \frac{\mathrm{d}}{\mathrm{d}t}\left(\pi r_{\mathrm{f}}^2 \int_0^{\ell} \frac{\sigma_{\mathrm{f}}^2}{2E_{\mathrm{f}}}\,\mathrm{d}z + 2\pi \int_0^{\ell}\int_{r_{\mathrm{f}}}^{R} \frac{\tau_m^2}{2G_m} r\,\mathrm{d}r\,\mathrm{d}z\right) + 2\pi \int_0^{\ell}\int_{r_{\mathrm{f}}}^{R} \tau_m \dot{\gamma}_m^{\mathrm{c}} r\,\mathrm{d}r\,\mathrm{d}z, \tag{45}$$

where λ indicates the pull-out displacement at $z = 0$, so that

$$\lambda = \int_0^{\ell} \frac{\sigma_{\mathrm{f}}}{E_{\mathrm{f}}}\,\mathrm{d}z. \tag{46}$$

Here it is noticed again that only shear is considered for the matrix in conformity with the shear lag assumption. Use of Eqs. (17) and (46) allows Eq. (45) to become

$$p_0 \int_0^{\ell} \frac{\dot{\sigma}_{\mathrm{f}}}{E_{\mathrm{f}}}\,\mathrm{d}z = \int_0^{\ell} \frac{\sigma_{\mathrm{f}}\dot{\sigma}_{\mathrm{f}}}{E_{\mathrm{f}}}\,\mathrm{d}z + \int_0^{\ell}\int_{r_{\mathrm{f}}}^{R} \frac{r_{\mathrm{f}}^2 \sigma_{\mathrm{f}}' \dot{\sigma}_{\mathrm{f}}'}{2G_m r}\,\mathrm{d}r\,\mathrm{d}z - \int_0^{\ell}\int_{r_{\mathrm{f}}}^{R} \sigma_{\mathrm{f}}' \dot{\gamma}_m^{\mathrm{c}}\,\mathrm{d}r\,\mathrm{d}z. \tag{47}$$

Then, it can be shown that substitution of the fiber stress profile (28) into Eq. (47) results in Eq. (32), which has led to the solutions (36a) and (36b). This means that the energy balance condition (44) and the bilinear fiber stress profile (28) also yield the solutions (36a) and (36b), and that the solutions (36a) and (36b) satisfy the energy balance condition (45).

For the fiber breakage model considered in Section 4.2, the elastic tensile energy in the fiber, the elastic shear energy in the matrix and the energy dissipation due to shear creep in the matrix are in equilibrium in the cell, because the lateral and end surfaces of the cell are subjected to fixed displacement $\varepsilon_0 z$. This energy balance is represented as Eq. (45) or Eq. (47) with $p_0 = 0$. Then, in the same way as in the fiber pull-out model, it can be shown that the solutions (43a) and (43b) satisfy the energy balance condition in the cell, and that the energy-balance based solution for the fiber breakage model in the previous work (Ohno and Miyake, 1999) is derivable from the variational method developed in the present work. In the previous work, however, the elastic strain in matrix and the radial variation of matrix shear stress were ignored. Hence, the solutions (43a) and (43b) are identical to the previous one, if the effect of the elastic strain in matrix is negligible and if the volume fraction of fibers is sufficiently high.

5. Discussion

We have derived the analytical solutions (36a), (36b), (43a) and (43b) by approximating bilinearly the profiles of fiber stress. It is seen that the solutions (36a) and (36b) with p_0 replaced by $E_{\mathrm{f}}\varepsilon_0$ is identical to Eqs. (43a) and (43b). In this section, to discuss the validity of the solutions, we compare Eqs. (36a) and (36b) with a finite difference computation and an experiment based on Raman spectroscopy.

5.1. Comparison of present solution and computation

Fig. 4(a) and (b) compare the solutions (36a) and (36b) with a finite difference computation of Eqs. (9) and (15). The computation has been done in the same way as in the work of Du and McMeeking (1995) by employing nondimensional quantities

$$\hat{r} = \frac{r}{r_{\mathrm{f}}}, \quad \hat{z} = \frac{z}{r_{\mathrm{f}}}, \quad \hat{t} = B_\tau E_{\mathrm{f}} p_0^{n-1} t, \quad \hat{\sigma}_{\mathrm{f}} = \frac{\sigma_{\mathrm{f}}}{p_0}. \tag{48}$$

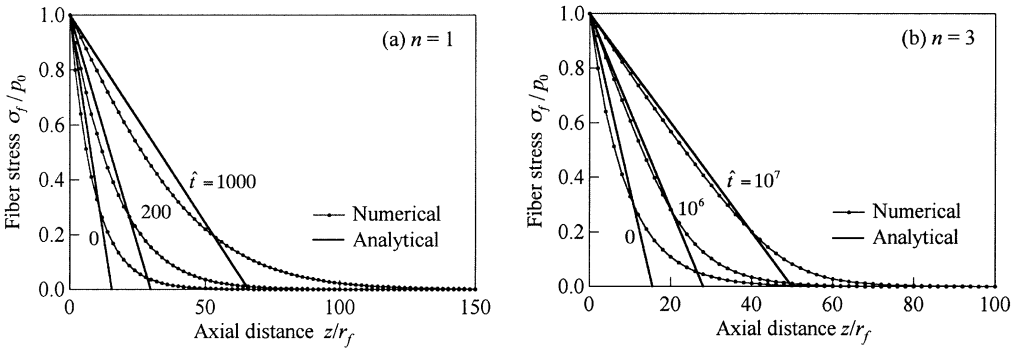

Fig. 4. Time-dependent profiles of fiber stress by analytical solution and finite difference computation ($G_m/E_f = 0.01$, $R/r_f = 5$, $\ell/r_f = 200$); (a) $n = 1$ and (b) $n = 3$.

Fig. 4(a) and (b) deal with linear and nonlinear cases of matrix creep, respectively; the material parameters employed are given in the figure caption. It is seen from the figures that, within the bilinear approximation of fiber stress profiles, the solutions (36a) and (36b) agree well with the computation in the two cases. Especially the solution (36b), which is for $n \geqslant 1$, works better, as seen in Fig. 4(b). This is because the nonlinearity of matrix shear creep gets fiber stress to distribute more bilinearly, as was found by Du and McMeeking (1995).

5.2. Effect of elastic shear deformation of matrix

Before moving on to the comparison with an experiment, we discuss the effect of the elastic shear deformation of matrix, which has been taken into account in the present work.

When $G_m = \infty$, we have $a(0) = 0$ from Eq. (39), and consequently the solutions (36a) and (36b) are reduced to

$$a(t) = r_f \left(3B_\tau E_f \ln \frac{R}{r_f} t \right)^{1/2}, \quad n = 1, \tag{49a}$$

$$a(t) = r_f \left\{ \frac{3(n+1)B_\tau E_f p_0^{n-1}}{2^n (n-1)} \left[1 - \left(\frac{r_f}{R} \right)^{n-1} \right] t \right\}^{1/(n+1)}, \quad n \neq 1. \tag{49b}$$

Hence, when $G_m = \infty$, the stress transfer length a develops from zero in proportion to $t^{1/(n+1)}$. This was the finding in the exact solution of Mason et al. (1992), who ignored the elastic shear strain in matrix in deriving their solution.

Fig. 5(a) and (b) illustrate the effect of the elastic shear strain of matrix on the time-dependent increase of a in the two cases of $n = 1$ and 3, respectively. As seen from the figures, $a(t)$ is larger just after loading if G_m/E_f is smaller. The dependence of $a(t)$ on G_m/E_f, however, fades with time, as was found numerically by Lagoudas et al. (1989). It is noticed that the solutions with $G_m = \infty$, Eqs. (49a) and (49b), become valid if these solutions get providing such a as comparable with $a(0)$ given by Eq. (39). Hence, we can say that the effect of the elastic shear strain of matrix cannot be ignored until matrix shear creep develops to be comparable with the initial elastic shear strain in matrix.

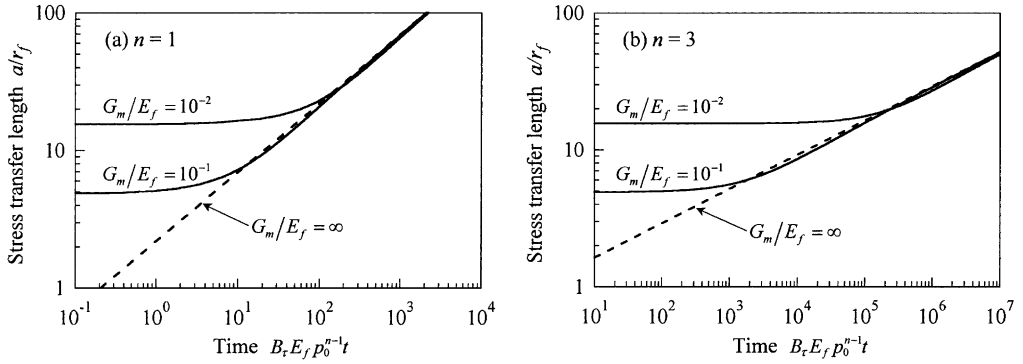

Fig. 5. Influence of matrix shear rigidity on time-dependent increase of stress transfer length; (a) $n = 1$, $R/r_f = 5$ and (b) $n = 3$, $R/r_f = 5$.

5.3. Comparison of present solution and experiment

Now let us apply the present solution to one of the fiber pull-out experiments done by Miyake et al. (2001). In the experiment, a single carbon fiber/acrylic model composite was employed, and one end of the carbon fiber was subjected to a constant stress of $p_0 = 2.7$ GPa for 500 h. Fig. 6 shows the fiber stress profiles measured using laser Raman spectroscopy in the experiment.

A notice is necessary for applying the present solution to the experiment mentioned above. It was concluded that the sliding at fiber/matrix interface occurred under the loading to $p_0 = 2.7$ GPa, since the maximum value of interfacial shear stress determined from the fiber stress profiles in Fig. 6 was only about one tenth of the theoretical estimation based on the perfect bonding at interface (Miyake et al., 2001). The sliding has not been taken into account in the preceding sections. Nevertheless, the functional (18) and the resulting solutions (36a) and (36b) remain valid, if the sliding took place *only initially* in the experiment, and if the initial value of a is taken to be equal to a slip length a_s, i.e.,

$$a(0) = a_s. \tag{50}$$

Using Eq. (4), a_s can be expressed in terms of interfacial slip stress τ_s as

$$a_s = \frac{r_f p_0}{2\tau_s}. \tag{51}$$

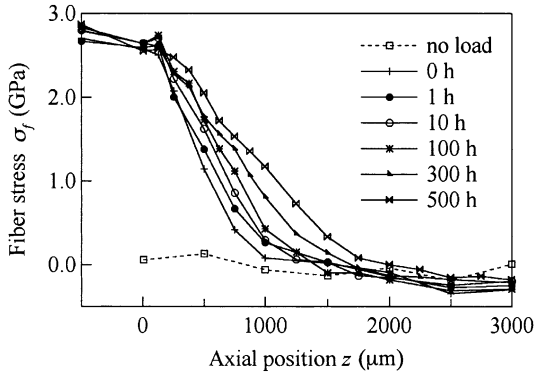

Fig. 6. Time-dependent change of fiber stress profile in single carbon fiber/acrylic model composite (Miyake et al., 2000).

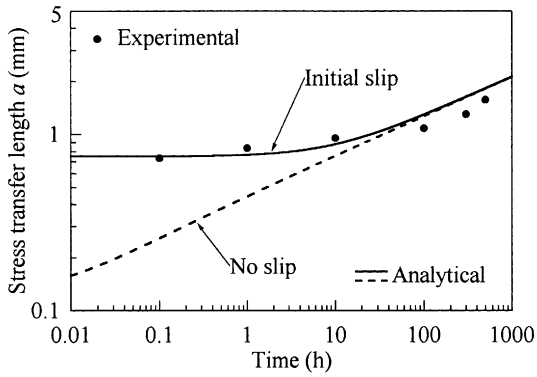

Fig. 7. Comparison of experiment and analytical solution based on creep constants determined by steady-state fitting of creep curves.

Fig. 7 compares the experiment and the solution (36b) with respect to $a(t)$. It is seen that the solution (36b) with the initial slip mentioned above agrees well with the experimental relation indicated by solid circles, which were determined by approximating bilinearly the fiber stress profiles in Fig. 6. The material constants used for the solution are given in Table 1. The value of R/r_f in the table was shown to be appropriate for a fiber embedded in infinite matrix by Li and Grubb (1994), and the creep constants were determined by fitting creep curves of the acrylic employed (Appendix A). Incidentally, R/r_f is ascertained to have negligible influence in Eq. (36b) on simulating the experiment, since R/r_f does not appear in $a(0)$ given by Eqs. (50) and (51).

The dashed line in Fig. 7 illustrates the prediction based on the perfect bonding at interface, i.e., the solution (36b) with $a(0)$ prescribed as Eq. (39). It is seen that this prediction fails to agree with the experiment up to $t \approx 10$ h. We are thus led to confirm that the assumption of the perfect bonding at interface is not appropriate for simulating the experiment.

The solution (36b) is based on Norton's law expressed as Eq. (33). As a consequence, the transient creep behavior of the matrix material is disregarded in the predictions shown in Fig. 7. Now, just for discussing the effect of such creep behavior, let us assume simply the time-hardening of matrix shear creep

$$\frac{\partial \gamma_m^c}{\partial t^*} = B_\tau^* |\tau_m|^{n-1} \tau_m, \quad t^* = t_0 \left(\frac{t}{t_0} \right)^k, \tag{52}$$

where B_τ^*, n, t_0 and k are material constants (see Table 1 and Appendix A). Then, we have the solution (36b) with t and B_τ replaced by t^* and B_τ^*, respectively. This solution gives the predictions shown in Fig. 8. It is seen that the predictions in this figure are a little better than those in Fig. 7. It is, however, not necessary to change the conclusions, which we have obtained by discussing the results in Fig. 7.

Table 1
Material constants

Elastic constants etc.,	$E_f = 490$ GPa, $G_m = 570$ MPa, $r_f = 2.7$ μm, $R/r_f = 4$
Matrix creep constants	
No hardening	$B_\tau = 1.25 \times 10^{-4}$ MPa^{-n} h^{-1}, $n = 3.5$
Time-hardening	$B_\tau^* = 1.25 \times 10^{-4}$ MPa^{-n} h^{-1}, $n = 3.5$, $t_0 = 50$ h, $k = 0.65$
Interfacial slip stress	$\tau_s = 4.9$ MPa

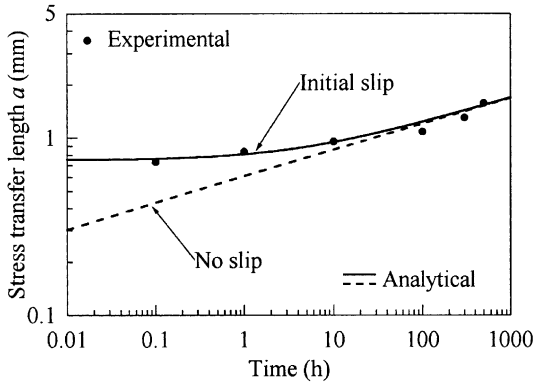

Fig. 8. Comparison of experiment and analytical solution with time-hardening of matrix creep.

6. Long-term creep rupture of unidirectional composites

Ohno and Miyake (1999) analyzed the long-term creep rupture of a unidirectional composite, with a fiber volume fraction V_f, subject to constant stress σ; they assumed the bilinear distribution of fiber stress and employed Curtin's (1991) model. In this section, the solutions (43a) and (43b) are applied to evaluating the characteristic time in their analysis.

Let us outline the analysis of Ohno and Miyake (1999). It was supposed that the fibers are brittle and have the scatter of tensile strength obeying the Weibull distribution with three parameters L_0, S_0 and m, and that interfacial sliding stress τ_s is low. It was assumed that the longitudinal normal stress in matrix, σ_m, is completely relaxed during long-term creep, i.e., $\sigma_m = 0$, giving rise to initial overall strain $\varepsilon^{\#} = \sigma/(V_f E_f)$ except for the effect of fiber breaks (Du and McMeeking, 1995). It was also assumed that all fiber breaks have the same amount of relaxation of interfacial shear stress τ_i as that around an initial break (Iyengar and Curtin, 1997). Then, Curtin's (1991) model led to

$$\frac{\sigma}{V_f} = E_f \varepsilon(t) \left\{ 1 - \frac{\tau_s}{2|\tau_i(t)|} \left[\frac{E_f \varepsilon(t)}{S_c} \right]^{m+1} \right\}, \tag{53}$$

where $S_c = (L_0 S_0^m \tau_s / r_f)^{1/(m+1)}$. Moreover, by noticing that the difference of rupture strain ε_r from $\varepsilon^{\#}$ is likely to be small in long-term creep, $|\tau_i(t)|$ in Eq. (53) was replaced with that under the relaxation at constant overall strain $\varepsilon^{\#}$. Thus, by considering the energy balance around an initial fiber break at constant overall strain $\varepsilon^{\#}$ and by ignoring the elastic strain in matrix as well as the radial variation of shear stress in matrix, $|\tau_i(t)|$ in Eq. (53) was set to be

$$|\tau_i(t)| = \tau_s \left[1 + (n+1) \frac{t}{t^{\#}} \right]^{-1/(n+1)}, \tag{54}$$

where $t^{\#}$ is a characteristic time. Then, by substituting Eq. (54) into Eq. (53), the strain and time at rupture were eventually obtained as follows:

$$\varepsilon_r = \frac{m+2}{m+1} \frac{\sigma}{V_f E_f}, \tag{55}$$

$$t_r = \frac{t^{\#}}{n+1} \left[\left(\frac{V_f S_{max}}{\sigma} \right)^{(m+1)(n+1)} - 1 \right], \tag{56}$$

where $S_{\max}$ represents the load carrying capacity of fibers in composites under tensile loading (Curtin, 1991):

$$S_{\max} = S_c \frac{m+1}{m+2}\left(\frac{2}{m+2}\right)^{1/(m+1)}. \tag{57}$$

Now we show that the solutions (43a) and (43b) allow $|\tau_i(t)|$ in Eq. (53) to be expressed as Eq. (54) as far as long-term creep is concerned. Let us suppose that the cell in the fiber breakage model is subject to constant overall strain $\varepsilon^{\#}$, and that the profile of fiber stress is bilinearly approximated. Then, Eqs. (4) and (40) with $\varepsilon_0 = \varepsilon^{\#}$ give

$$|\tau_i(t)| = \frac{r_f E_f \varepsilon^{\#}}{2a(t)}. \tag{58}$$

Since $\varepsilon^{\#} = \sigma/(V_f E_f)$, the above equation is rewritten as

$$|\tau_i(t)| = \tau_s \frac{a(0)}{a(t)}, \tag{59}$$

where $a(0)$ is equal to the interfacial slip length caused by τ_s under $\sigma_m = 0$, i.e.,

$$a(0) = \frac{r_f \sigma}{2V_f \tau_s}. \tag{60}$$

Since the effect of elastic shear strain in matrix fades with time (Section 5.2), Eqs. (43a), (43b), (59) and (60) provide Eq. (54) with

$$t^{\#} = \frac{\sigma^2}{6E_f B_\tau \tau_s^2 V_f^2 \ln(R/r_f)}, \quad n = 1, \tag{61a}$$

$$t^{\#} = \frac{(n-1)\sigma^2}{6E_f B_\tau \tau_s^{n+1} V_f^2 \left[1 - (r_f/R)^{n-1}\right]}, \quad n \neq 1. \tag{61b}$$

Here, $B_\tau = 3^{(n+1)/2} B_\sigma$ if based on the Mises equivalence of tension and torsion (see Appendix A), and $R/r_f = 2(V_f^{\max}/V_f)^{1/2} - 1$ for the hexagonal array of fibers, where $V_f^{\max}$ $(= \pi/2\sqrt{3})$ indicates the maximum value of V_f.

Ohno and Miyake (1999) determined $t^{\#}$ from the solution of τ_i based on the energy balance in the cell, though they ignored the radial variation of matrix shear stress and the elastic shear strain in matrix. Let us remember that the present solutions (43a) and (43b) also satisfy the energy balance in the cell (Section 4.3), and that the effect of elastic shear strain in matrix has been neglected in deriving Eqs. (61a) and (61b). Therefore, except for the effect of the radial variation of matrix shear stress, $t^{\#}$ in the present work agrees with the previous one. In other words, as V_f approaches $V_f^{\max}$, the two results become identical with each other; but if $V_f \ll V_f^{\max}$, the present result can be better than the previous one.

7. Conclusions

The present work dealt with a variational method to analyze the time-dependent change in fiber stress profiles in unidirectional fibrous composites; two kinds of axisymmetric models, i.e., fiber breakage and fiber pull-out models, were considered. A functional based on incremental complementary energy was demonstrated and proved to have the stationary function satisfying a differential equation based on the shear lag assumption. Then, analytical solutions were derived by assuming bilinear profiles of fiber stress and by getting the functional stationary; a power law of matrix shear creep was employed to derive the analytical solutions. It was shown that the resulting solutions satisfy an energy balance condition and agree

well with a finite-difference computation of the differential equation. It was thus found that the energy-balance based solution obtained by Ohno and Miyake (1999) is derivable from the variational method developed in the present work, and that the elastic deformation of matrix has significant influence on the time-dependent increase of the stress transfer length until time elapses sufficiently long. It was also shown that the solution for the fiber pull-out model simulates well the experiment on a carbon fiber/acrylic model composite if the initial slip at fiber/matrix interface is taken into account. In addition, the solution for the fiber breakage model was used for evaluating the characteristic time in long-term creep rupture of uni-directional composite.

The present work has the following merits in comparison to the previous work (Ohno and Miyake, 1999). First, a variational method based on incremental complementary energy was developed in the present work. Such a variational method is based on the well-established principle and therefore can be effective even when assumed solutions have multiple unknowns; the Rayleigh–Ritz method can be used to determine the multiple unknowns from the stationary condition. This is in contrast to the energy approach considered in the previous work, which provides just one equation and consequently allows only one unknown to be determined. The variational method developed in the present work thus can be more general and opens the way to considering other problems such as multifiber systems containing single or multiple fiber breaks. Second, both the fiber pull-out and fiber breakage models were studied in the present work, while only the fiber breakage model in the previous work. The fiber pull-out model is important especially for the purpose of utilizing laser Raman spectroscopy for observing the effect of matrix creep on fiber stress profiles. Third, the radial variation of matrix shear stress as well as the elastic strain in matrix was taken into account in the present work, so that the present solution can be valid for single-fiber model composites or composites with low volume fractions of fibers.

Acknowledgements

This work was supported in part by the Ministry of Education under a Grant-in-Aid for Scientific Research C (no. 11650086).

Appendix A

Fig. 9 shows tensile creep curves of the acrylic employed by Miyake et al. (2001). The dashed lines in the figure indicate the simulation based on

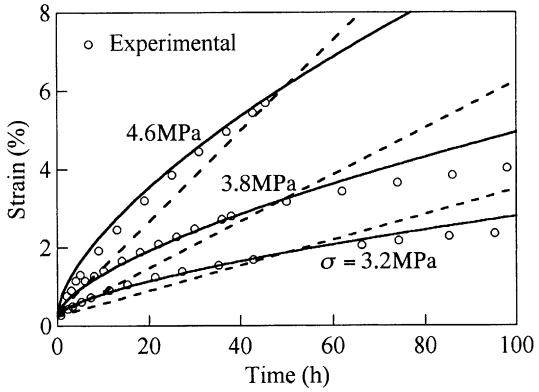

Fig. 9. Tensile creep curves of acrylic at constant stresses; dashed and solid lines fitted with Eqs. (A.1) and (A.2), respectively.

$$\varepsilon = \frac{\sigma}{E_m} + B_\sigma \sigma^n t, \tag{A.1}$$

where $B_\sigma = 5.53 \times 10^{-6}$ (MPa^{-n} h^{-1}) and $n = 3.5$. The solid lines, on the other hand, are based on

$$\varepsilon = \frac{\sigma}{E_m} + B_\sigma^* \sigma^n t^*, \quad t^* = t_0 \left(\frac{t}{t_0} \right)^k, \tag{A.2}$$

where $B_\sigma^* = 5.53 \times 10^{-6}$ (MPa^{-n} h^{-1}), $n = 3.5$, $t_0 = 50$ (h) and $k = 0.65$.

The equivalence between tension and torsion ascertained for inelastic deformation of metals tends to hold for polymers as well (Kitagawa et al., 1992; Qiu and Kitagawa, 1993). Hence, if we assume simply the Tresca equivalence, B_τ in Eq. (33) and B_τ^* in Eq. (52) satisfy $B_\tau = 2^{n+1} B_\sigma$ and $B_\tau^* = 2^{n+1} B_\sigma^*$, respectively, so that we have the creep constants given in Table 1.

References

Clyne, T.W., Withers, P.J., 1993. An Introduction to Metal Matrix Composites. Cambridge University Press, pp. 20–24.

Cox, H.L., 1952. The elasticity and strength of paper and other fibrous materials. Br. J. Appl. Phys. 3, 72–79.

Curtin, W.A., 1991. Theory of mechanical properties of ceramic-matrix composites. J. Am. Ceram. Soc. 74, 2837–2845.

Du, Z.-Z., McMeeking, R.M., 1995. Creep models for metal matrix composites with long brittle fibers. J. Mech. Phys. Solids 43, 701–726.

Iyengar, N., Curtin, W.A., 1997. Time-dependent failure in fiber-reinforced composites by means of matrix and interface shear creep. Acta Mater. 45, 3419–3429.

Kitagawa, M., Onoda, T., Mizutani, K., 1992. Stress–strain behavior at finite strains for various strain paths in polyethylene. J. Mater. Sci. 27, 13–23.

Lagoudas, D.C., Hui, C.-Y., Phoenix, S.L., 1989. Time evolution of overstress profiles near broken fibers in a composite with a viscoelastic matrix. Int. J. Solids Struct. 25, 45–66.

Li, Z.-F., Grubb, D.T., 1994. Single-fibre polymer composites, part I: interfacial shear strength and stress distribution in the pull-out test. J. Mater. Sci. 29, 189–202.

Lifshitz, J.M., Rotem, A., 1970. Time-dependent longitudinal strength of unidirectional fibrous composites. Fibre Sci. Tech. 3, 1–20.

Mason, D.D., Hui, C.-Y., Phoenix, S.L., 1992. Stress profiles around a fiber break in a composite with a nonlinear, power law creeping matrix. Int. J. Solids Struct. 29, 2829–2854.

Miyake, T., Yamakawa, T., Ohno, N., 1998. Measurement of stress relaxation in broken fibers embedded in epoxy using Raman spectroscopy. J. Mater. Sci. 33, 5177–5183.

Miyake, T., Kokawa, S., Ohno, N., Biwa, S., 2001. Evaluation of time-dependent change in fiber stress profiles during long-term pull-out tests at constant loads using Raman spectroscopy. J. Mater. Sci., in press.

Ohno, N., Miyake, T., 1999. Stress relaxation in broken fibers in unidirectional composites: modeling and application to creep rupture analysis. Int. J. Plasticity 15, 167–189.

Ohno, N., Okamoto, N., Miyake, T., Nishide, S., Masaki Jr., S., 1994a. Acoustic emission and fiber damage in creep of a unidirectional SCS-6/Ti-15-3 metal matrix composite at 450°C. Scripta Metall. Mater. 31, 1549–1554.

Ohno, N., Toyoda, K., Okamato, N., Miyake, T., Nishide, S., 1994b. Creep behavior of a unidirectional SCS-6/Ti-15-3 metal matrix composite at 450°C. ASME J. Engng. Mater. Technol. 116, 208–214.

Otani, H., Phoenix, S.L., Petrina, P., 1991. Matrix effects on lifetime statistics for carbon fibre-epoxy microcomposites in creep rupture. J. Mater. Sci. 26, 1955–1970.

Phoenix, S.L., Schwartz, P., Robionson IV, H.H., 1988. Statistics for the strength and lifetime in creep-rupture of model carbon/epoxy composites. Compos. Sci. Technol. 32, 81–120.

Qiu, J., Kitagawa, M., 1993. Cyclic stress–strain curves of polyoximethylene under combined tension-torsion. Trans. Jpn. Soc. Mech. Engng. A/59, 2926–2933 (in Japanese).